RESEARCH ARTICLE

Human Mutation

OFFICIAL JOURNAL
HGVS
HUMAN GENOME VARIATION SOCIETY
www.hgvs.org

RyR1 Deficiency in Congenital Myopathies Disrupts Excitation–Contraction Coupling

Haiyan Zhou,[1] Ori Rokach,[2] Lucy Feng,[1] Iulia Munteanu,[1] Kamel Mamchaoui,[3] Jo M. Wilmshurst,[4] Caroline Sewry,[1] Adnan Y. Manzur,[1] Komala Pillay,[5] Vincent Mouly,[2] Michael Duchen,[6] Heinz Jungbluth,[7,8,9] Susan Treves,[2,10]* and Francesco Muntoni[1]*

[1]Dubowitz Neuromuscular Centre, Institute of Child Health, University College London, London, UK; [2]Department of Anaesthesia and Biomedicine, Basel University and University Hospital Basel, Basel, Switzerland; [3]UM76 Université Pierre et Marie Curie, UMRS974 INSERM, UMR 7215 CNRS, Institut de Myologie AIM, Groupe hospitalier Pitié-Salpétrière, 47 bd de l'Hôpital, Paris, France; [4]Department of Paediatric Neurology, School of Child and Adolescent Health, University of Cape Town, Red Cross Children's Hospital, Cape Town, South Africa; [5]Department of Paediatric Pathology, School of Child and Adolescent Health, University of Cape Town, Red Cross Children's Hospital, Cape Town, South Africa; [6]Cell and Developmental Biology, University College London, London, UK; [7]Department of Paediatric Neurology, Evelina Children's Hospital, London, UK; [8]Clinical Neuroscience Division, IoP, King's College, London, UK; [9]Randall Division of Cell and Molecular Biophysics, Muscle Signalling Group King's College London, London, UK; [10]Department of Life Sciences, University of Ferrara, Ferrara, Italy

Communicated by María-Jesús Sobrido

Received 19 October 2012; accepted revised manuscript 18 March 2013.
Published online 29 March 2013 in Wiley Online Library (www.wiley.com/humanmutation). DOI: 10.1002/humu.22326

ABSTRACT: In skeletal muscle, excitation–contraction (EC) coupling is the process whereby the voltage-gated dihydropyridine receptor (DHPR) located on the transverse tubules activates calcium release from the sarcoplasmic reticulum by activating ryanodine receptor (RyR1) Ca^{2+} channels located on the terminal cisternae. This subcellular membrane specialization is necessary for proper intracellular signaling and any alterations in its architecture may lead to neuromuscular disorders. In this study, we present evidence that patients with recessive *RYR1*-related congenital myopathies due to primary RyR1 deficiency also exhibit downregulation of the alfa 1 subunit of the DHPR and show disruption of the spatial organization of the EC coupling machinery. We created a cellular RyR1 knockdown model using immortalized human myoblasts transfected with RyR1 siRNA and confirm that knocking down RyR1 concomitantly downregulates not only the DHPR but also the expression of other proteins involved in EC coupling. Unexpectedly, this was paralleled by the upregulation of inositol-1,4,5-triphosphate receptors; functionally however, upregulation of the latter Ca^{2+} channels did not compensate for the lack of RyR1-mediated Ca^{2+} release. These results indicate that in some patients, RyR1 deficiency concomitantly alters the expression pattern of several proteins involved in calcium homeostasis and that this may influence the manifestation of these diseases.

Hum Mutat 34:986–996, 2013. © 2013 Wiley Periodicals, Inc.

KEY WORDS: ryanodine receptor; dihydropyridine; RYR1; congenital myopathies

Introduction

The precise regulation of intracellular calcium homeostasis is critical for normal skeletal muscle development and function. Excitation–contraction (EC) coupling requires the correct assembly, distribution, and interaction of a number of proteins residing in the sarcoplasmic reticulum (SR), the organelle of striated muscle dedicated to calcium homeostasis. Two key elements involved in calcium release are the voltage-gated dihydropyridine receptor (DHPR; MIM #114208), located on the transverse tubules, and the ryanodine receptor (RyR1; MIM #180901), the principal calcium release channel of skeletal muscle situated in the terminal cisternae of the SR [Nakai et al., 1996]. The predicted structure of the RyR1 suggests that the calcium release pore is located in the C-terminal domain of the protein, whereas the N-terminal domain constitutes the foot structure that interacts with DHPR [Dulhunty and Pouliquin, 2003; Ramachandran et al., 2009; Van Petegem, 2012]. The direct physical interaction between DHPR and RyR1 is essential for skeletal muscle EC coupling and any alterations in the subcellular distribution of proteins or membranes involved EC coupling can lead to impaired muscle function [Oddoux et al., 2009; Pan et al., 2002].

Disturbance of calcium homeostasis due to defects in RyR1 is the underlying feature of the malignant hyperthermia susceptibility (MIM #145600) trait, a pharmacogenetic reaction to volatile anesthetics and muscle relaxants, and a wide range of

Additional Supporting Information may be found in the online version of this article.

*Correspondence to: Francesco Muntoni, Dubowitz Neuromuscular Centre, Institute of Child Health, University College London, London WC1N 1EH, UK. E-mail: f.muntoni@ucl.ac.uk; Susan Treves, Department of Anaesthesia and Biomedicine, Basel University and University Hospital Basel, Basel 4031, Switzerland. E-mail: susan.treves@unibas.ch

Contract grant sponsors: Muscular Dystrophy Association (Grant number 174047); the Wellcome Trust Value in People (Grant code FPEG); the SNF (grant N° 3100 030_129785); AFM; the 7th FP EC network MYOAGE (Contract 223576); Botnar Stiftung; MRC Neuromuscular Centre to the Biobank; the Great Ormond Street Hospital Children's Charity.

congenital myopathy phenotypes, including dominantly inherited central core disease (CCD; MIM #117000) and recessively inherited multiminicore disease (MIM #255320) with or without opthalmoplegia [Jungbluth et al., 2002; 2005; Quane et al., 1993; Zhou et al., 2006; 2007], subgroups of centronuclear myopathy, congenital fiber type disproportion, and the King-Denborough Syndrome [Clarke et al., 2010; Dowling et al., 2011; Jungbluth et al., 2007; Wilmshurst et al., 2010]. Although dominantly inherited *RYR1*-related congenital myopathies have been extensively studied and are usually attributed to RyR1 channels that are either "leaky" or show impaired calcium conductance [Dirksen and Avila, 2002; Treves et al., 2008], the pathogenesis of recessively inherited *RYR1*-related myopathies is not well understood, though a decrease in RyR1 protein content has been reported in muscle biopsies from some patients [Wilmshurst et al., 2010; Zhou et al., 2007]. Besides mutations in the *RYR1*, substitutions in other genes linked to neuromuscular disorders, encoding proteins involved in EC coupling have so far been reported only for *CACNA1*, the gene encoding the alfa 1 subunit of the DHPR ($Ca_v1.1$) in patients with malignant hyperthermia [Monnier et al., 1997; Pirone et al., 2010; Toppin et al., 2010]. We recently reported that a patient with periodic paralysis who harbored recessively inherited *RYR1* mutations [Zhou et al., 2010] with no *CACNA1S* mutation, had a marked reduction of RyR1 protein and a disruption of RyR1/$Ca_v1.1$ colocalization, indicating potential secondary effects of certain *RYR1* mutations on key proteins of the EC coupling machinery.

In the present investigation, we extended these findings and report abnormal expression and distribution of $Ca_v1.1$ in muscle biopsies from a number of patients with recessive *RYR1* mutations with reduced RyR1 content. Mimicking RyR1 depletion in human myotubes using a *RYR1* siRNA knockdown approach caused a decrease in $Ca_v1.1$ with a concomitant upregulation of inositol-1,4,5-trisphosphate receptors (IP3R; MIM #147265). These results provide new insights into the pathogenesis of recessive *RYR1*-related myopathies with primary RyR1 deficiency.

Materials and Methods

Muscle Biopsies

Studies on muscle biopsies from patients were approved by the author's Institutional Ethical Committee and conducted under the Declaration of Helsinki. Patients were encoded to protect their confidentiality, and written informed consent obtained. Routine histopathological studies were performed according to standard procedures. All patients presented in this study have a clear clinical and histological diagnosis of a congenital myopathy, and were molecularly diagnosed as having *RYR1* mutations. Control muscle biopsies were from donors with no neuromuscular diseases. RNA samples were studied in nineteen patients and nine controls; immunohistochemical studies were performed in four patients and three controls; Western blot studies were performed in two patients and three controls.

Molecular Genetics

The genetic information of all patients was taken from the genetic reports. The *RYR1* nucleotide numbering is based on transcript variant NM_00540.2, where the nucleotide numbering reflects cDNA numbering with +1 corresponding to the A of the ATG translation initiation codon in the reference sequence, according to journal guidelines (www.hgvs.org/mutnomen). The initiation codon is codon 1. The variants reported have been submitted to the Leiden RYR1 locus specific database (http://www.lovd.nl/RYR1).

Immortalization and Culture of Skeletal Muscle Cell Line

Human satellite cells were derived from the skeletal muscle biopsy of a 19-year-old female donor with no neuromuscular disorder. Skeletal muscle cell line immortalization was performed as previously described [Mamchaoui et al., 2011; Zhu et al., 2007]. Briefly, cultured cells were double transfected by recombinant retroviruses containing the telomerase (hTERT) cDNA and Cdk4 cDNA, followed by clonal selection of myogenic lines. Immortalized myoblasts were maintained in skeletal muscle cell growth medium (PromoCell, Heidelberg, Germany) in low oxygen atmosphere (5% O_2 and 5% CO_2) at 37°C.

Immunofluorescence

All cryosections from muscle biopsies were cut at a thickness of 8 μm for immunohistochemistry. Sections were incubated with primary antibodies at room temperature for 1 hr, washed in 0.1 M PBS pH 7.2 and incubated with secondary antibody conjugated to Alexa 488 and biotinylated secondary antibody for 1 hr at room temperature, followed by thorough rinsing in PBS. After washing, muscle sections were incubated with streptavidin conjugated to Alexa 594 for 15 min at room temperature then washed and mounted using Hydromount mounting medium (National Diagnostics, Georgia, USA). Images were digitally captured using Metamorph software. For immunofluorescence on myotubes, glass coverslip grown cells were fixed for 30 min in 3.7% paraformaldehyde in PBS; cells were rinsed with PBS and permeabilized with 1% Triton X-100 in PBS for 30 min. After incubation with blocking buffer (1% blocking buffer, Roche, in PBS) for 60 min at room temperature, slides were processed as described above. The primary antibodies used for immunohistochemistry were mouse anti-RyR1 monoclonal antibody (1:500; Abcam, Cambridge, UK), goat anti- $Ca_v1.1$ polyclonal antibody (1:200; Santa Cruz, Texas, USA), and rabbit anti-ß-tubulin (1:20; Santa Cruz, Texas, USA).

cDNA Synthesis and Quantitative Real-Time PCR

Total RNA was extracted from muscle biopsies using the RNeasy kit (Qiagen, Crawley, UK); 500 ng of each RNA sample was used for first-strand cDNA synthesis with Superscript III reverse transcription kit (Invitrogen, Paisley, UK). Quantitative real-time PCR products of *RYR1*, *CACNA1S*, and *DES* were amplified with the TaqMan universal PCR Master Mix (Applied Biosystems, Leusden, Netherlands). Samples were incubated in a 25 μl reaction mix according to manufacturer's instructions. Quantitative real-time PCR was performed using Applied Biosystem fast 7500 Real Time PCR System using the recommended program: activation at 50°C for 2 min and 95°C for 10 min, 40 cycles of 95°C for 15 sec and 60°C for 1 min. Quantification was based on the comparative ΔΔCt method. One of the samples treated with negative control siRNA was used to calibrate the data and to analyze results. For *ITPR1*, *ITPR2*, and *ITPR3* quantitative real-time PCR samples were amplified with MESA Blue qPCR kit (Eurogentec, Seraing, Belgium). Gene specific qPCR primers, including *ITPR1*, *ITPR2*, *ITPR3*, *GAPDH*, and *DES*, were commercially available from Qiagen. Samples were incubated in a 25 μl reaction mix according to manufacturer's instructions. Quantitative real-time PCR was performed using Applied Biosystem fast 7500 Real Time PCR System using the recommended program: activation at 95°C for 5 min, 40 cycles of 95°C for 3 sec, and 60°C

for 1 min. Quantification was based on concurrent standard curves produced from serial dilutions of control cDNA from untreated cultured myotubes. *DES* and *GAPDH* were used as internal reference genes. The expression of *ITPRs* in cultured myotubes or muscle biopsies were normalized by DES or GAPDH, and calibrated by taking the ratio of one of the control samples as 1.0. Total RNA was extracted from human myotubes using Trizol (Invitrogen, Lucerne, Switzerland) and cDNA synthesized with the High Capacity cDNA synthesis kit from Applied Biosystem and the following primers: MYH 1-Myosin heavy chain, forward: 5′ GGG AGA CCT AAA ATT GGC TCA A 3′, reverse: 5′ TTG CAG ACC GCT CAT TTC AAA 3′; TNNT1—Troponin T1, forward: 5′ TGA TCC CGC CAA AGA TCC C 3′, reverse: 5′ TCT TCC GCT GCT CGA AAT GTA 3′; DAG1—Dystroglycan 1, forward: 5′ AGC AAA GGA TTG ACC TCC TGC 3′, reverse: 5′ CCA CCG GCA CTA ATT TCA TGT T 3′; Desmin, forward: 5′ AAC CAG GAG TTT CTG ACC ACG 3′, reverse: 5′ TTG AGC CGG TTC ACT TCG G 3′; GAPDH, forward: 5′ CTG GGC TAC ACT GAG CAC C 3′, reverse: 5′AAG TGG TCG TTG AGG GCA ATG 3′. As well as the ITPR primers described above. Transcript levels were normalized to GAPDH expression levels.

Western Blotting

Total protein was extracted from cells lysates or frozen skeletal muscle sections in sampling buffer consisting of 75 mM Tris–HCl, 1% SDS, and cocktail of protease inhibitor (Roche, Burgess Hill, UK). Protein concentration was quantified by the BCA protein assay kit (Pierce, Rockford, IL, USA). Thirty micrograms of proteins were loaded and separated using NuPAGE Precast gels (3%–8% Tris–acetate; Invitrogen) and then transferred electrophoretically to nitrocellulose membrane (GE Healthcare, Buckinghamshire, UK). The membrane was blocked with 5% goat serum (Sigma, Dorset, UK) in PBS buffer with 0.5% Tween-20 (PBS-T) and then probed with primary antibodies at room temperature for 1 hr or 4°C overnight. After washing in PBS-T, membranes were incubated with HRP-antimouse or HRP-antirabbit IgG (the Jackson Laboratory, West Grove, PA, USA; 1:50,000) for 1 hr at room temperature. Immunoreactivity was visualized using enhanced chemiluminescence detection kit (GE Healthcare). Semi-quantification of the bands was performed by densitometric analysis and data was processed using the Image J software.

The primary antibodies used in this study include mouse monoclonal anti-RyR1 (Abcam; 1:2,500), rabbit anti-$Ca_v1.1$ (Santa Cruz; 1:1,000), mouse monoclonal-antidesmin (DAKO, Glostrup, Denmark; 1:2,000), mouse monoclonal anti-IP3R III (BD, Devon UK; 1:1,000), mouse monoclonal anti-SERCA2 antibody (Abcam; 1:1,000), mouse monoclonal anti-α-actinin 2 (Sigma; 1:20,000), and mouse monoclonal anti-β-tubulin (Sigma; 1:4,000).

RYR1 Knockdown by siRNA

Immortalized myoblasts obtained as described above (immortalization and culture human skeletal muscle cell line) were seeded on 30 mm diameter plates at a density of 5–8 $\times$ 10^5 cells per well in order to be confluent by the next day. *RYR1* siRNA (Santa Cruz Biotechnology) was transfected using lipofectamine 2000 in OptiMEM medium following the manufacturer's recommendations (Invitrogen). A series of concentrations [10, 30, and 50 nM] of siRNA were tested and cells treated with the same concentrations of negative siRNA were used as control. The transfection medium was changed to differentiation medium (PromoCell) 6 hr after transfection and changed thereafter every 2 days; cells visibly started to fuse 4–5 days after transfection/differentiation, and myotubes were collected at day 7.

Intracellular Calcium Measurements

Myotubes, mock transfected or transfected with 50 nM siRNA, were either untreated or treated with 1 μM Xestospongin C (Sigma chemicals, St. Gallen, Switzerland) for 40 min during fura-2 (final concentration was 5 μM) loading. Cells were rinsed one time with Krebs-Ringer and then coverslips were mounted onto a 37°C thermostated chamber which was continuously perfused with Krebs-Ringer medium; individual cells were stimulated with the indicated agonists (60 mM KCl, 600 μM 4-chloro-*m*-cresol, 100 μM ATP) made up in Krebs-Ringer containing no added Ca^{2+} plus 100 μM La^{3+} in order to monitor changes in the cytoplasmic calcium concentration due to release from intracellular stores, by means of a 12-way 100 mm diameter quartz micromanifold computer-controlled microperfuser (ALA Scientific Instruments, Farmingdale, NY, USA), as previously described [Ducreux et al., 2004]. On-line measurements were recorded using a fluorescent Axiovert S100 TV inverted microscope (Carl Zeiss GmbH, Jena, Germany) equipped with a 20× water-immersion FLUAR objective (0.17 NA), filters (BP 340/380, FT 425, BP 500/530) and attached to a Cascade 125+ CCD camera. Changes in the free cytosolic calcium concentration were analyzed using MetaMorph (Molecular Devices) imaging system and the average pixel value for each cell was measured as previously described [Ducreux et al., 2004; Treves et al., 2010].

Statistical Analysis

Statistical analysis was performed using the Student's *t*-test for comparison of two samples or the ANOVA test for comparison of multiple data, followed by the Bonferroni's post hoc test. GraphPad Prism 5 and Origin softwares were used for statistical analysis and graph design.

Results

RyR1 and DHPR Expression and Distribution in Skeletal Muscle Biopsies from Patients Carrying *RYR1* Mutations

Figure 1 shows immunohistochemical staining on skeletal muscle biopsies from three patients carrying recessive *RYR1* mutations, one patient carrying a dominant *RYR1* mutation and one control individual. A summary of the clinical and histopathological features and genetic details of the patients is given in Supp. Table S1. Patient 1 carried the heterozygous mutations p.R109W+p.M485V in one allele and the missense plus nonsense mutations p.D708N+p.R2241X in the other allele; patient 2 carried the heterozygous p.E879K mutation in one allele and the splice site mutation c.3381+1G>A in the other allele. Patient 3 carried the dominant *RYR1* mutation p.G4638D and patient 4 carried the homozygous missense mutation p.R3772Q. No additional mutations were found after screening the entire *RYR1* coding region of each patient. Biopsies from patients 3 and 4, where histopathology showed typical central or eccentric cores on NADH staining, showed the same patterns of distribution of DHPR and RyR1 in a rim around the core area (Fig. 1). On the other hand, a segregated distribution of RyR1 and DHPR was observed in muscle sections from patients 1 and 2, in whom histopathology showed the characteristic multi-mini cores on NADH staining, there was distinct aggregation of the DHPR in some of the muscle fibers in associated with reduction of RyR1 staining.

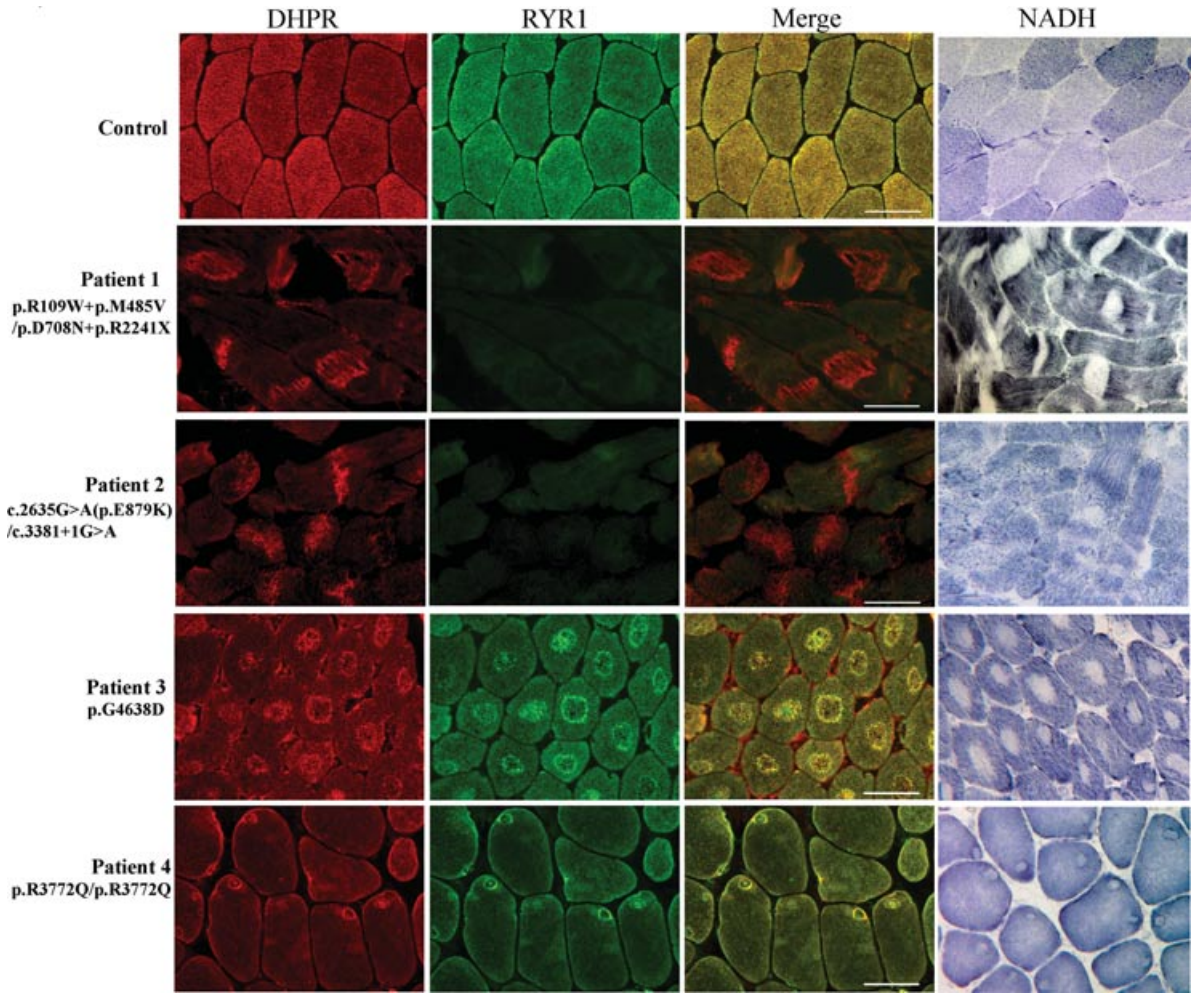

Figure 1. Protein expression of RyR1 and DHPR in muscle biopsy of patients with different *RYR1* mutations. Double staining of RyR1 and DHPR, and NADH staining in muscle biopsies of patients with congenital myopathy and *RYR1* mutations. NADH staining was performed in non-serial sections from RyR1/DHPR double staining. Scale bar = 25 μm.

RYR1 but Not *CACNA1S* Transcript is Reduced in Skeletal Muscle from Patients Carrying Recessive *RYR1* Mutations

To investigate changes in *RYR1* expression at the transcriptional level, we performed quantitative real-time PCR of *RYR1* in patient's muscle biopsies, using *DES* as the skeletal muscle specific reference gene. RNA samples extracted from muscle biopsies of 19 patients with confirmed *RYR1* mutations were collected for this study. Patients were arranged into three groups according to the types of mutations. *RYR1*-AD group consisted of six patients carrying dominant *RYR1* mutations; *RYR1*-R1 group included four patients with recessive homozygous or compound heterozygous missense mutations; and *RYR1*-R2 group included nine patients carrying heterozygous recessive mutations in which one allele contained a missense mutation, and the other a loss of function mutation. We also included biopsies from nine normal control individuals in the control group. The relative expression of *RYR1* was 0.89 ± 0.07 in the control group, 0.83 ± 0.10 in the *RYR1*-AD group, 0.61 ± 0.07 in the *RYR1*-R1 group and 0.57 ± 0.06 in the *RYR1*-R2 group (Fig. 2A). Significant reduction of *RYR1* mRNA transcripts was observed in *RYR1*-R1 and *RYR1*-R2 groups, where patients were affected by recessive mutations on both alleles, compared with control group (P = 0.0035 between *RYR1*-R2 and control; P = 0.044 between *RYR1*-R1 and control). No difference was observed in patients carrying dominant *RYR1* mutations (*RYR1*-AD) compared with control group. *CACNA1S* mRNA was also measured by quantitative real-time but no significant difference was observed in its transcription level in muscle biopsies between mutation groups and controls (Fig. 2B).

We further investigated the effects of RyR1 depletion by performing RyR1 knockdown experiments on an immortalized human muscle cell line, using *RYR1* siRNA. Seven days after transfection and differentiation, once visible multinucleated myotubes appeared, *RYR1* mRNA was quantified by real-time PCR. As shown in Figure 3A the *RYR1* transcript was reduced in a siRNA concentration-dependent manner. The relative expression of *RYR1* mRNA was: 0.47 ± 0.09 for the 10 nM siRYR1 group; 0.31 ± 0.03 for the 30 nM siRYR1 group and 0.23 ± 0.03 for the 50 nM siRYR1 group compared with the control group (1.0 ± 0.0). In the same samples, the relative expression of *CACNA1S* (Fig. 3B) and *DES* (Fig. 3C) were not significantly changed.

Downregulation of RyR1 by siRNA did not affect myotube differentiation; indeed mean myotube diameter as well as the relative expression of differentiation-related markers such as dystroglycan 1 (DAG), myosin heavy chain 1 (MHC1), troponin T1 (TNNT1), and desmin (DES) [Galbiati et al., 1999; Trendelensburg et al.,

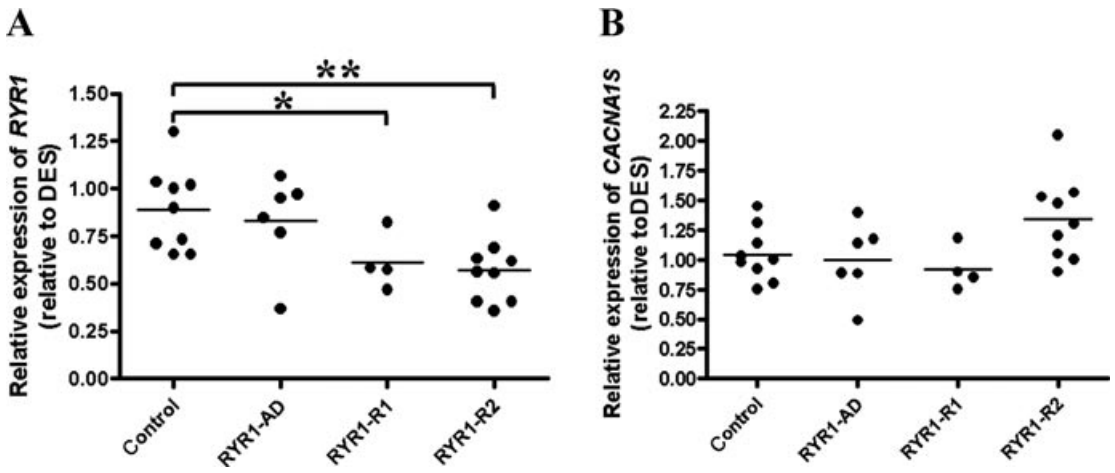

Figure 2. Quantitative reverse transcriptional real-time PCR of *RYR1* and *CACNA1S* in skeletal muscle biopsies from patients carrying different *RYR1* mutations. The relative content of *RYR1* and *CACNA1S* mRNA was assessed by real-time PCR using $\Delta\Delta$Ct method and using *DES* as muscle specific reference gene. The relative expression of *RYR1* and *CACNA1S* to *DES* in one of the control individuals was set as 1.0, and was used to calibrate the values of all other samples. Each symbol represents an individual and the bar indicates mean relative expression. ANOVA was used for the statistical analysis of the values in different groups, followed by the Bonferroni post statistics test. **A:** Relative expression of *RYR1* transcript in muscle biopsies. **B:** Relative expression of *CACNA1S* transcript in muscle biopsies. $^{*}P < 0.05$, $^{**}P < 0.01$.

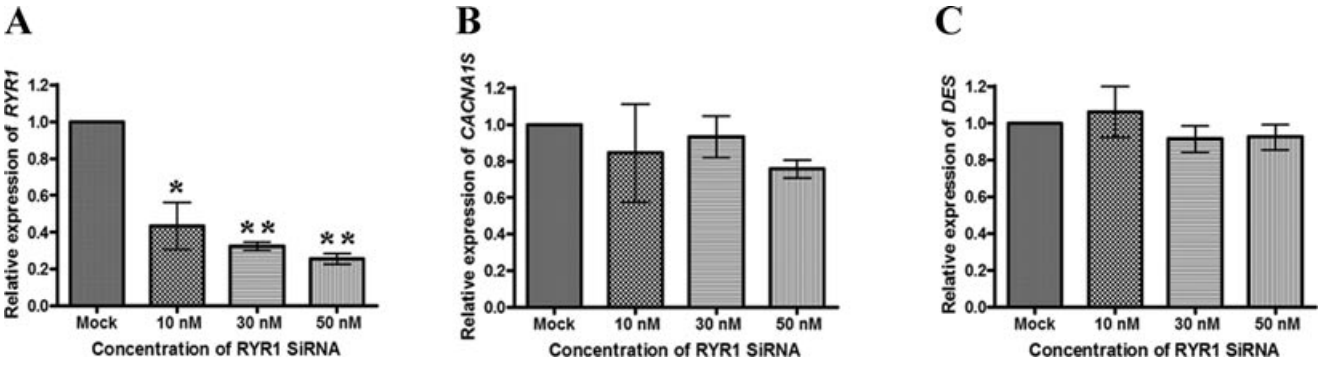

Figure 3. *RYR1*, *CACNA1S*, and DES mRNA expression in myotubes treated with *RYR1* siRNA. The relative quantification of *RYR1* (**A**), *CACNA1S* (**B**), and *DES* (**C**) mRNA was performed by quantitative real-time PCR. The value was obtained from three independent transfection experiments of myotubes treated with *RYR1* siRNA at concentrations of 10, 30, and 50 nM. The data are presented as mean ± SEM, $N = 3$. ANOVA was used for the statistical analysis of the values in the *RYR1* siRNA-treated myotubes to negative control siRNA, followed by Bonferroni post statistics test. The relative expression of target genes in control siRNA-treated myotubes was set as 1.0, and was used to normalize the values in the *RYR1* siRNA-treated myotubes. $^{*}P < 0.05$, $^{**}P < 0.01$.

2009] were similar in control and *RYR1* siRNA transfected myotubes (Fig. 4).

RyR1 Deficiency Affects $Ca_v1.1$ Content

We next assessed if the decrease in mRNA in siRNA transfected immortalized cells was paralleled by a decrease in protein content. Figure 5A shows a representative western blot performed seven days after treatment and Figure 5B shows the mean (±SEM) protein content in control versus siRNA-treated myotubes. As shown desmin and tubulin content were not affected by *RYR1* siRNA but there was a >50% decrease in RyR1, $Ca_v1.1$, SERCA2, and α-actinin content as assessed by western blotting in myotubes transfected with 50 nM *RYR1* siRNA. Unexpectedly, the relative content of IP3RIII, the other intracellular Ca^{2+} release channel of ER membranes was increased by approximately twofold.

The protein content of $Ca_v1.1$, SERCA2, α-actinin2, and IP3RIII were also assessed in the muscle biopsies from patients with RyR1 deficiency due to recessive mutations. Western blotting was performed on protein extracted from the muscle biopsies of two patients and three normal controls. The immunohistochemical staining of RyR1 and DHPR of patient 2 was shown in Figure 1; the double staining of RyR1 and DHPR in patient 5 has been previously reported [Zhou et al., 2010], with similar distribution pattern as shown in Figure 1.

Representative blots from patients and controls are shown in Figure 5C. There was a significant reduction of both RyR1 and DHPR proteins in the samples from the patients compared with controls ($N = 3$) (Fig. 5D). Significant upregulation of IP3R III (approximately twofold) was also observed in patients' muscle biopsies compared with the controls (Fig. 5D). However, no changes in SERCA2 and α-actinin 2 protein was observed in the patients' muscle biopsies samples.

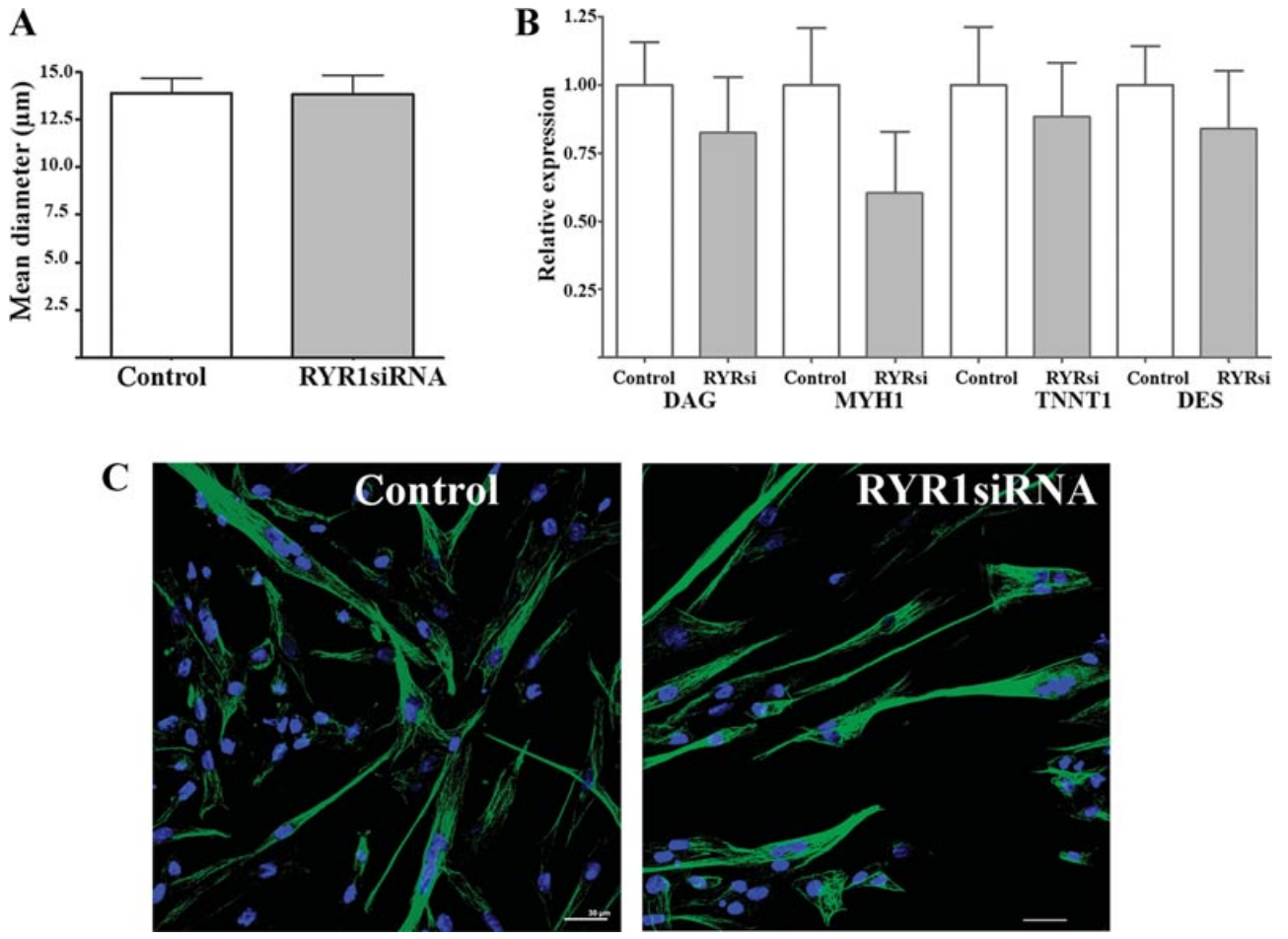

Figure 4. Downregulation of RyR1 by *RYR1* siRNA transfection does not affect myotube differentiation: Cells were transfected with 50 nM *RYR1* siRNA, differentiated for 5 days and then stained with β-tubulin and DAPI, the diameter of myotubes with >3 nuclei were measured and averagedconsidered. **A**: Mean ($\pm$SE) myotube diameter (μm) of 30 transfected and 30 mock transfected myotubes. (**B**: Relative mRNA expression of differentiation-related markers; *Dystroglycan* 1 (*DAG*), *Myosin heavy chain 1* (*MYH1*), *Troponin T1* (*TNNT1*), and *Desmin* (*DES*) normalized to *GAPDH* expression as internal control ($N = 6$). **C**: Immunofluorescentce of transfected (RYR1siRNA) or mock transfected (control) myotubes stained with anti- β tubulin (green) and DAPI and observed with a Nikon A1R confocal microscope with a 40$\times$ NeoFluar objective (1.4 NA). Bar indicates 30 μm.

All Three Types of *ITPRs* Transcripts are Upregulated in *RYR*1 Knockdown Myotubes and in Skeletal Muscles from Patients with Primary RyR1 Deficiency

The transcripts of all three isoforms of Inositol-1,4,5- Triphosphate Receptor (IP3R) genes (*ITPR1*, *ITPR2*, and *ITPR3*) were quantified by real-time RT-PCR in myotubes treated by *RYR1* siRNA. Significant upregulation of all three isoforms of ITPRs was observed in the *RYR1* knocked-down group compared with the control group (Fig. 6A). We then analyzed *ITPRs* transcripts in skeletal muscle from controls (N = 7), from patients with dominant *RYR1* mutations (N = 5) and from patients with heterozygous recessive *RYR1* mutations and RyR1 protein deficiency (N = 6). To ensure that the observed alterations were not due to heterogeneous tissue composition of the biopsies due to variable degrees of fibrosis or connective tissue accumulation, we used both the ubiquitous housekeeping gene *GAPDH* and muscle specific *DES* gene as internal reference genes. Irrespective of whether the analysis was made using *GAPDH* (Fig. 6B) or *DES* (Fig. 6C), patients with recessive *RYR1* mutations showed significant upregulations of all three IP3R transcripts, compared with the control group. No significant differences in *ITPR1*, *ITPR2*, and *ITP3R* expression were observed between the group of patients harboring dominant *RYR1* mutations and the control group, except for a patient carrying the dominant mutation p.R4861C, who showed unusually high levels of *ITPRs* expression. Interestingly, although this mutation was identified as de novo and was not found in either parent, the case was initially considered a recessive core myopathy because of the severe clinical features of the patient and the abnormality observed in parent's muscle biopsy [Manzur et al., 1998]. Unfortunately, the muscle biopsy failed western blotting RyR1 protein quantification due to sampling problems. In order to rule out the presence of other allelic mutations, we performed genomic analysis of the entire coding region and exon/intron boundaries of the *RYR1* gene; no other pathogenic variants were identified in this patient suggesting that in this patient the p.R4861C mutation is responsible for the pathological phenotype.

Taken together these results confirm that RyR1 deficiency induced in vitro as well as RyR1 protein deficiency occurring in vivo due to recessive *RYR1* mutations cause the upregulation of *ITPRs* transcripts.

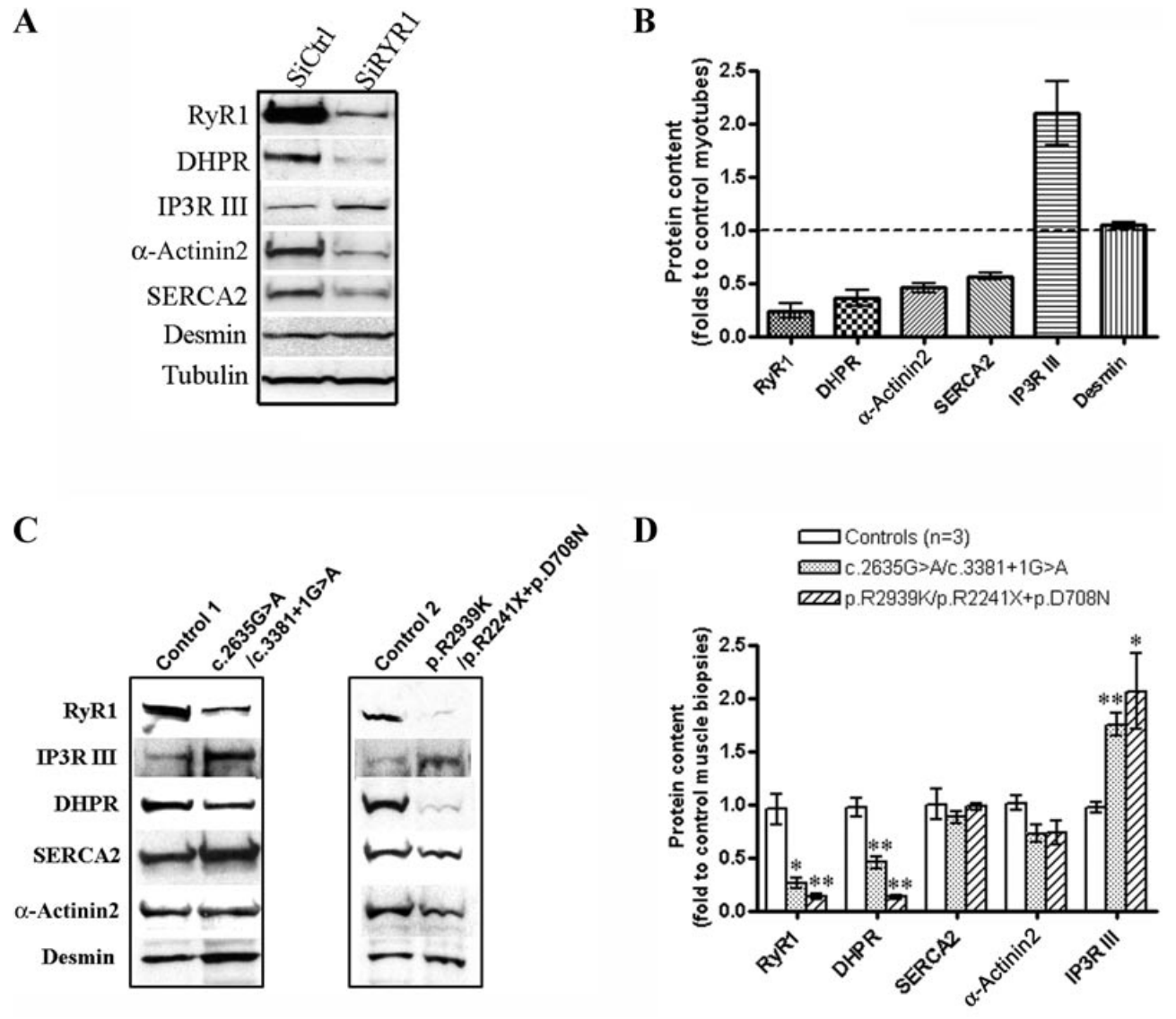

Figure 5. RyR1, DHPR, and other SR protein in *RYR1* siRNA-treated myotubes and muscle biopsies from patients with RyR1 deficiency due to recessive *RYR1* mutations. **A**: Representative western blots of RyR1, DHPR, IP3R-III, α-actinin 2, SERCA 2, desmin, and β-tubulin in human myotubes treated by *RYR1* siRNA. **B**: Semi-quantification of proteins in *RYR1* siRNA-treated myotubes. The expression of proteins was normalized to tubulin. Protein content in *RYR1* siRNA-treated group was compared with the control group. **C**: Representative western blots of RyR1, DHPR, IP3R-III, α-actinin 2, SERCA 2, and desmin in muscle biopsies from two patients (patient 2 and 5 in Supp. Table S1) with recessive RYR1 mutations. **D**: Semi-quantification of proteins in two patients, with RyR1 deficiency due to recessive *RYR1* mutations, and three controls. The expression of proteins was normalized by desmin.

Changes in Intracellular Ca^{2+} Homeostasis in *RYR1* Knocked-Down Myotubes

Using the human muscle cell line we assessed how downregulation of RyR1 by siRNA affects calcium homeostasis. Besides the resting [Ca^{2+}] and the size ionomycin sensitive Ca^{2+} stores, we measured several parameters, including the response (expressed as area under the curve, which more accurately reflects the total amount of Ca^{2+} released) of myotubes to KCl-induced depolarization, to pharmacological activation of RyR1 with 4-chloro-m-cresol and to ATP stimulation (which measures Ca^{2+} release via IP3R) in control cells, control cells treated with the IP3R inhibitor Xestospongin C and in RYR1 siRNA-treated cells (± Xestospongin C). This approach allows us to evaluate if the decrease in Ca^{2+} released due to downregulation of RyR1 could be compensated by upregulation of IP3R-mediated Ca^{2+} release. Figure 7 shows that RyR1 activation either directly by the addition of 600 μM 4-chloro-m-cresol or indirectly, by the addition of 60 mM KCl induces a large Ca^{2+} release that is independent of IP3Rs since the same amount of Ca^{2+} was released whether cells had been pre-treated or not with Xestospongin C. Downregulation of *RYR1* by 50 nM siRNA caused a threefold decrease of Ca^{2+} release by 4-cmc and KCl that was unaffected by Xestospongin C. Addition of 100 μM ATP (1) caused the release of approximately 50% of the Ca^{2+} compared with the release obtained by RyR1 activation, (2) was inhibited by Xestospongin C and importantly, (3) was unaffected by downregulation of *RYR1*. Downregulation of RyR1 affected neither the resting [Ca^{2+}] nor the total amount of ionomycin-induced Ca^{2+}-release, indicating no significant effect on the size of the intracellular

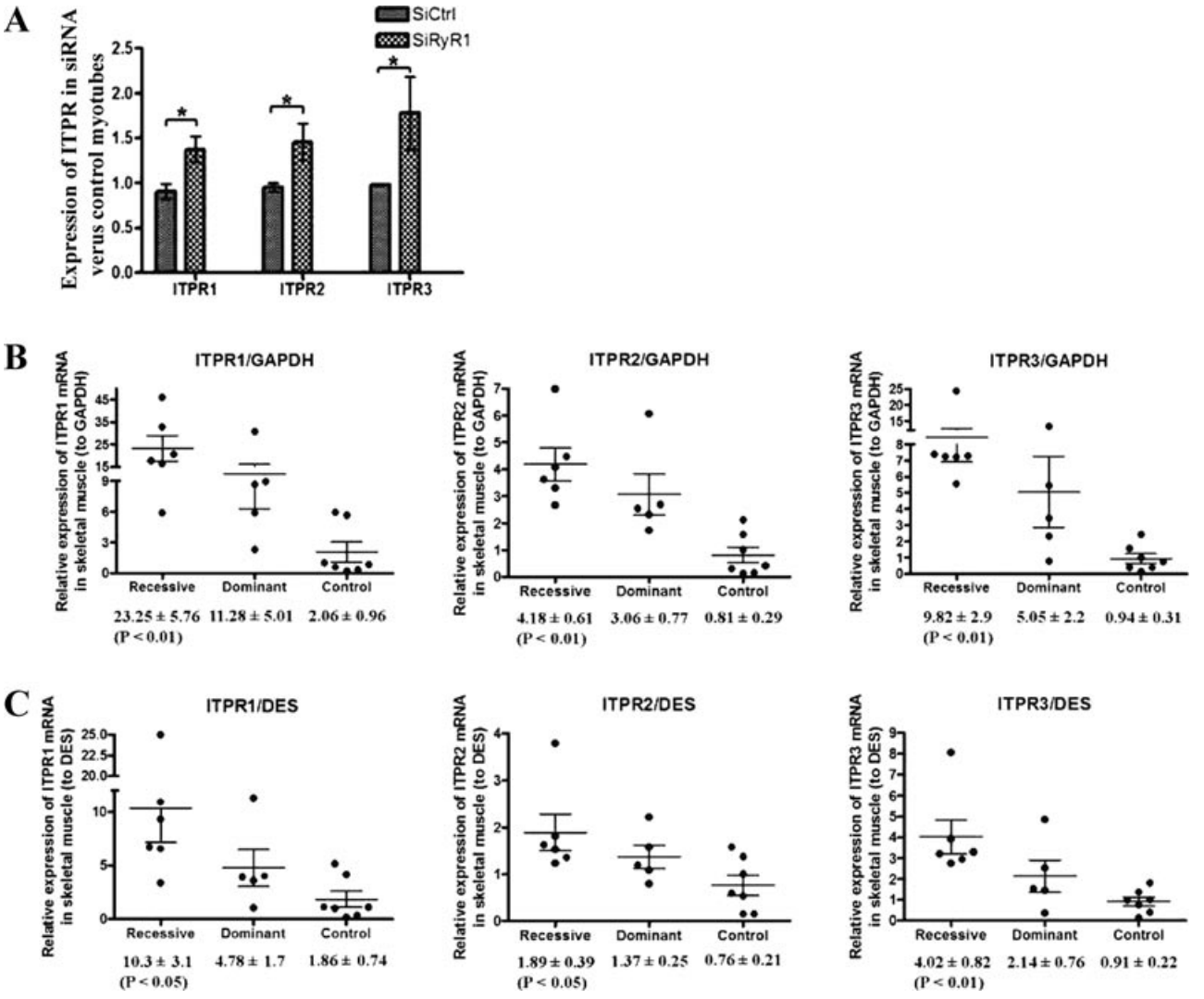

Figure 6. The expression of *ITPR1, ITPR2,* and *ITPR3* mRNA in RYR1 siRNA-treated myotubes and skeletal muscle biopsies from patients with different *RYR1* mutations. **A**: The relative expression of *ITPRs* mRNA in cultured myotubes treated with siRNA was measured by quantitative reverse transcript real-time PCR. Data are presented as mean ± SEM. $N = 4$ samples per group. $^*P < 0.05$. **B**: The relative expression of *ITPRs* mRNA measured by quantitative real-time PCR in skeletal muscle biopsies from controls ($N = 7$), patients with dominant *RYR1* mutations ($N = 5$) and patients with complex recessive *RYR1* mutations with RyR1 protein deficiency ($N = 6$). *GAPDH* was used as general internal control gene. **C**: The relative expression of *ITPRs* mRNA measured by quantitative real-time PCR in skeletal muscle biopsies by using *DES* as muscle-specific internal control gene.

Ca^{2+} stores. These results indicate that upregulation of IP3R does not functionally compensate the decreased Ca^{2+}-release due to the lower levels of RyR1 protein content.

Discussion

RYR1-related disorders with mainly dominant inheritance and normal RyR1 protein expression have been extensively studied at the functional level, whereas the mechanisms underlying *RYR1*-related myopathies with recessive inheritance and RyR1 deficiency remain only partially understood. Functional studies of common dominant *RYR1* mutations associated with CCD indicate two principal mechanisms associated with disturbed function of the mutant RyR1 channel, namely presence of a 'leaky channels' associated with reduction of SR calcium stores [Lynch et al., 1999], or "uncoupled" channels with muscle weakness resulting from a reduced capacity of RyR1 to transport Ca^2 [Avila et al., 2001]. In the present study, we report that recessive *RYR1* mutations associated with RyR1 deficiency are also responsible for EC uncoupling by negatively affecting DHPR-RyR1 colocalization in skeletal muscle. Indeed, this kind of EC uncoupling was initially reported in two animal models of *RYR1*-related disorders, the sporadic zebrafish *relatively relaxed* mutant with marked reduction of functional RyR1 protein [Hirata et al., 2007], and in *Ryr1* knockout (dyspedic) mice which do not express any ryanodine receptor 1 [Takeshima et al., 1994]. In dyspedic myotubes cultured from *Ryr1* knockout mice, there is no EC coupling, whereas introduction of exogenous RyR1 restores EC coupling and increases the density of the L-type Ca^{2+} current toward normal [Nakai et al., 1996]. The dependence of physiological EC coupling on correct mechanical coupling is also indicated by ultrastructural studies demonstrating the importance of a tight alignment of RyR tetramers on the junctional face membrane and of DHPR molecules (a tetrad) on the opposing T-tubule membrane [Block et al., 1988].

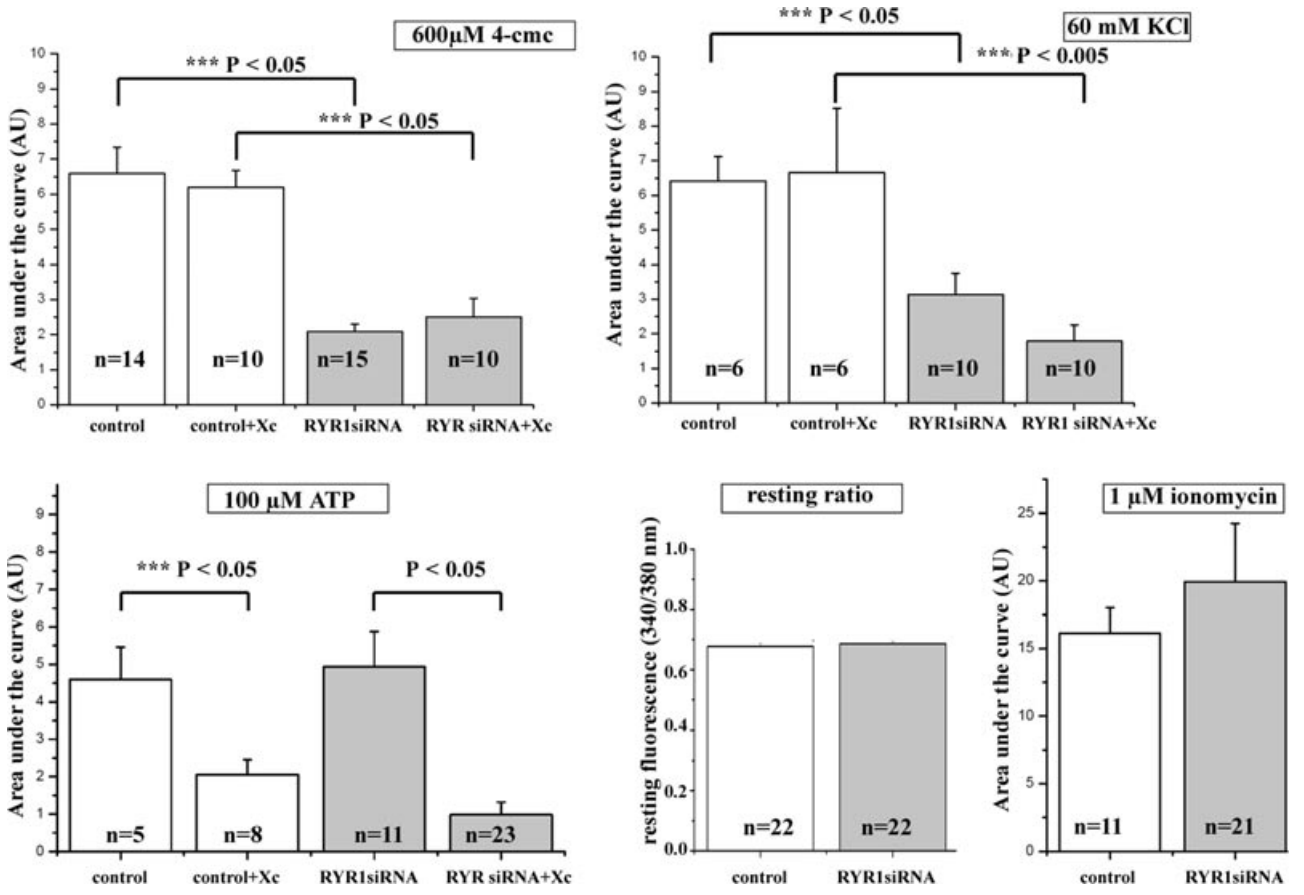

Figure 7. Analysis of calcium regulation in a human muscle cell line after transfection with *RYR1* siRNA. Cells were transfected with 50 nM RYR1 siRNA or mock transfected as described in the *Materials and Methods* section and were either untreated or treated with 1 µM Xestospongin C during the 40 min of fura-2 loading. Myotubes were stimulated with the indicated agonist in Krebs-Ringer containing no added Ca^{2+} plus 100 µM La^{3+} and the total amount of calcium released was calculated using Origin software by calculating the total transient, i.e. the area under the curve. Resting [Ca^{2+}] is presented as fluorescence ratio (340/380 nm) (au) before cell stimulation in Krebs-Ringer containing 2 mM Ca^{2+}; the total amount of rapidly releasable Ca^{2+} present in the SR/ER stores was obtained by calculating the area under the curve after exposing cells to 1 µM ionomycin in the Krebs-Ringer containing no added Ca^{2+} plus 0.5 mM EGTA. For details see *Materials and Methods* section. All results are expressed as mean value (±SEM) of the indicated number of cells. White bars mock transfected cells, grey bars cells transfected with *RYR1* siRNA. Statistical analysis was performed using Student's *t*-test.

Interestingly, depletion of RyR1 in vitro by siRNA in an immortalized human muscle cell line caused a decrease of $Ca_v1.1$ content, suggesting that proper alignment between the two calcium channels is required for the stability of the complex. Diminishment of $Ca_v1.1$ content has also been reported in dyspedic mouse skeletal muscle [Buck et al., 1997] and in one previous immunohistochemical study on core myopathies, in which a patient exhibiting virtual absence of RyR1 showed focal accumulation of DHPR within or around the cores [Herasse et al., 2007]. The loss of DHPR/RyR1 colocalization strongly suggests a physical EC uncoupling in patients with some recessive *RYR1* mutations. We suggest that the characteristic staining pattern of $Ca_v1.1$ may be a useful immunohistochemical indicator to select patients for *RYR1* sequencing, currently still very costly and time consuming due to the large size of the gene.

Aside the downregulation of $Ca_v1.1$, we observed downregulation of SERCA2 and alfa-actinin in RyR1 knocked-down myotubes. This is in contrast to the upregulation of SERCA reported in dyspedic myotubes [Eltit et al., 2010; 2011] and to the lack of changes in SERCA2 and alfa-actinin protein levels in the patient's biopsies. Opposing effects on SERCA2 expression have been reported in C_2C_{12} cells transfected with two different *RYR1* mutations. Vega et al. (2011) reported that transfection with the *RYR1* Y523S MH-linked mutation caused an increase in SERCA2 expression whereas transfection of C2C12 cells with the CCD-linked I4897T *RYR1* mutation caused its downregulation. Furthermore, they also reported that the expression of a particular mutant affects the degree of myotube differentiation, in that C2C12 cells transfected with the RyR1 cDNA harboring the I4897T mutation were similar to control myotubes in size and fusion index 8 days after differentiation, whereas cells transfected with the RyR1 cDNA harboring the Y523S substitution were larger than control myotubes [Vega et al., 2011]. We did not find any significant differences in size and in the expression of differentiation-related markers such as dystroglycan 1, troponin T1, myosin heavy chain, and desmin [Galbiati et al., 1999; Trendelenburg et al., 2009] in RYR1siRNA transfected and control cells. Thus, knocking down a protein in vitro does not mimic all aspects of what happens in vivo in muscles of patients harboring recessive mutations causing RyR1 depletion and further experiments are required to understand the mechanisms involved in the reciprocal regulation of SR proteins.

In the present study, we demonstrate that in human skeletal muscle under conditions of RyR1 deficiency, IP3R are upregulated. In

cultured mouse skeletal muscle cells IP3R predominantly expressed around the nuclear envelope, are mainly associated with slow Ca^{2+} transients and appear to be involved in the regulation of gene expression [Jaimovich et al., 2000; Jaimovich and Carrasco, 2002]. The IP3/IP3R-induced calcium signal plays little or no substantial role in skeletal muscle EC coupling under physiological conditions [Posterino and Lamb, 1998] and as shown in the present study, upregulation of IP3R in RyR1-deficient states does not compensate for the physical collapse of the EC coupling machinery. Nevertheless, the IP3/IP3R pathway may be involved in slow calcium release leading to activation of expression of certain genes and the present study indicates the possible existence of a complex interplay of RyR1 and IP3R signaling pathways.

In conclusion, our results demonstrate upregulation of an alternative calcium regulating system via IP3R in recessive *RYR1*-related myopathies with RyR1 deficiency, and indicate the potential importance of the IP3R signaling cascade in the pathophysiology of these neuromuscular disorders. Future studies aimed at determining the role of the IP3R system in RyR1-deficient congenital myopathies and its correlation with disease progression could provide further insight into the pathogenesis of this condition.

Acknowledgments

We would like to thank Mr Darren Chambers for muscle biopsy processing in this study. In addition the authors would like to acknowledge the platform for culture and immortalization of the Myology Institute in Paris (France).

Disclosure statement: The authors declare no conflict of interest.

References

Avila G, O'Brien JJ, Dirksen RT. 2001. Excitation–contraction uncoupling by a human central core disease mutation in the ryanodine receptor. Proc Natl Acad Sci USA 98:4215–4220.

Block BA, Imagawa T, Campbell KP, Franzini-Armstrong C. 1988. Structural evidence for direct interaction between the molecular components of the transverse tubule/sarcoplasmic reticulum junction in skeletal muscle. J Cell Biol 107:2587–2600.

Buck ED, Nguyen HT, Pessah IN, Allen PD. 1997. Dyspedic mouse skeletal muscle expresses major elements of the triadic junction but lacks detectable ryanodine receptor protein and function. J Biol Chem 272:7360–7367.

Clarke NF, Waddell LB, Cooper ST, Perry M, Smith RL, Kornberg AJ, Muntoni F, Lillis S, Straub V, Bushby K, Guglieri M, King MD, et al. 2010. Recessive mutations in RYR1 are a common cause of congenital fiber type disproportion. Hum Mutat 31:E1544–E1550.

Dirksen RT, Avila G. 2002. Altered ryanodine receptor function in central core disease: leaky or uncoupled Ca(2+) release channels? Trends Cardiovasc Med 12:189–197.

Dowling JJ, Lillis S, Amburgey K, Zhou H, Al-Sarraj S, Buk SJ, Wraige E, Chow G, Abbs S, Leber S, Lachlan K, Baralle D, et al. 2011. King-Denborough syndrome with and without mutations in the skeletal muscle ryanodine receptor (RYR1) gene. Neuromuscul Disord 21:420–427.

Ducreux S, Zorzato F, Muller C, Sewry C, Muntoni F, Quinlivan R, Restagno G, Girard T, Treves S. 2004. Effect of ryanodine receptor mutations on interleukin-6 release and intracellular calcium homeostasis in human myotubes from malignant hyperthermia-susceptible individuals and patients affected by central core disease. J Biol Chem 279:43838–43846.

Dulhunty AF, Pouliquin P. 2003. What we don't know about the structure of ryanodine receptor calcium release channels. Clin Exp Pharmacol Physiol 30:713–723.

Eltit JM, Li H, Ward CW, Molinski T, Pessah IN, Allen PD, Lopez JR. 2011. Orthograde dihydropyridine receptor signal regulates ryanodine receptor passive leak. Proc Natl Acad Sci USA 108:7046–7051.

Eltit JM, Yang T, Li H, Molinski TF, Pessah IN, Allen PD, Lopez JR. 2010. RyR1-mediated Ca^{2+} leak and Ca^{2+} entry determine resting intracellular Ca^{2+} in skeletal myotubes. J Biol Chem 285:13781–13787.

Galbiati F, Volonté D, Engelman JA, Scherer PE, Linsanti MP. 1999. Targeted downregulation of caveolin-3 is sufficient to inhibit myotube formation in differentiating C2C12 myoblasts. J Biol Chem 274: 30315–30321.

Herasse M, Parain K, Marty I, Monnier N, Kaindl AM, Leroy JP, Richard P, Lunardi J, Romero NB, Ferreiro A. 2007. Abnormal distribution of calcium-handling proteins: a novel distinctive marker in core myopathies. J Neuropathol Exp Neurol 66:57–65.

Hirata H, Watanabe T, Hatakeyama J, Sprague SM, Saint-Amant L, Nagashima A, Cui WW, Zhou W, Kuwada JY. 2007. Zebrafish relatively relaxed mutants have a ryanodine receptor defect, show slow swimming and provide a model of multi-minicore disease. Development 134:2771–2781.

Jaimovich E, Carrasco MA. 2002. IP3 dependent Ca^{2+} signals in muscle cells are involved in regulation of gene expression. Biol Res 35:195–202.

Jaimovich E, Reyes R, Liberona JL, Powell JA. 2000. IP(3) receptors, IP(3) transients, and nucleus-associated Ca(2+) signals in cultured skeletal muscle. Am J Physiol Cell Physiol 278:C998–C1010.

Jungbluth H, Muller CR, Halliger-Keller B, Brockington M, Brown SC, Feng L, Chattopadhyay A, Mercuri E, Manzur AY, Ferreiro A, Laing NG, Davis MR, et al. 2002. Autosomal recessive inheritance of RYR1 mutations in a congenital myopathy with cores. Neurology 59:284–287.

Jungbluth H, Zhou H, Hartley L, Halliger-Keller B, Messina S, Longman C, Brockington M, Robb SA, Straub V, Voit T, Swash M, Ferreiro A, et al. 2005. Minicore myopathy with ophthalmoplegia caused by mutations in the ryanodine receptor type 1 gene. Neurology 65:1930–1935.

Jungbluth H, Zhou H, Sewry CA, Robb S, Treves S, Bitoun M, Guicheney P, Buj-Bello A, Bonnemann C, Muntoni F. 2007. Centronuclear myopathy due to a de novo dominant mutation in the skeletal muscle ryanodine receptor (RYR1) gene. Neuromuscul Disord 17:338–345.

Lynch PJ, Tong J, Lehane M, Mallet A, Giblin L, Heffron JJ, Vaughan P, Zafra G, MacLennan DH, McCarthy TV. 1999. A mutation in the transmembrane/luminal domain of the ryanodine receptor is associated with abnormal Ca^{2+} release channel function and severe central core disease. Proc Natl Acad Sci USA 96:4164–4169.

Mamchaoui K, Trollet C, Bigot A, Negroni E, Chaouch S, Wolff A, Kandalla PK, Marie S, Di SJ, St Guily JL, Muntoni F, Kim J, et al. 2011. Immortalized pathological human myoblasts: towards a universal tool for the study of neuromuscular disorders. Skelet Muscle 1:34.

Manzur AY, Sewry CA, Ziprin J, Dubowitz V, Muntoni F. 1998. A severe clinical and pathological variant of central core disease with possible autosomal recessive inheritance. Neuromuscul Disord 8:467–473.

Monnier N, Procaccio V, Stieglitz P, Lunardi J. 1997. Malignant-hyperthermia susceptibility is associated with a mutation of the alpha 1-subunit of the human dihydropyridine-sensitive L-type voltage-dependent calcium-channel receptor in skeletal muscle. Am J Hum Genet 60:1316–1325.

Nakai J, Dirksen RT, Nguyen HT, Pessah IN, Beam KG, Allen PD. 1996. Enhanced dihydropyridine receptor channel activity in the presence of ryanodine receptor. Nature 380:72–75.

Oddoux S, Brocard J, Schweitzer A, Szentesi P, Giannesini B, Brocard J, Faure J, Pernet-Gallay K, Bendahan D, Lunardi J, Csernoch L, Marty I. 2009. Triadin deletion induces impaired skeletal muscle function. J Biol Chem 284:34918–34929.

Pan Z, Yang D, Nagaraj RY, Nosek TA, Nishi M, Takeshima H, Cheng H, Ma J. 2002. Dysfunction of store-operated calcium channel in muscle cells lacking mg29. Nat Cell Biol 4:379–383.

Pirone A, Schredelseker J, Tuluc P, Gravino E, Fortunato G, Flucher BE, Carsana A, Salvatore F, Grabner M. 2010. Identification and functional characterization of malignant hyperthermia mutation T1354S in the outer pore of the Cavalpha1S-subunit. Am J Physiol Cell Physiol 299:C1345–C1354.

Posterino GS, Lamb GD. 1998. Investigation of the effect of inositol trisphosphate in skinned skeletal muscle fibres with functional excitation–contraction coupling. J Muscle Res Cell Motil 19:67–74.

Quane KA, Healy JM, Keating KE, Manning BM, Couch FJ, Palmucci LM, Doriguzzi C, Fagerlund TH, Berg K, Ording H. 1993. Mutations in the ryanodine receptor gene in central core disease and malignant hyperthermia. Nat Genet 5:51–55.

Ramachandran S, Serohijos AW, Xu L, Meissner G, Dokholyan NV. 2009. A structural model of the pore-forming region of the skeletal muscle ryanodine receptor (RyR1). PLoS Comput Biol 5:e1000367.

Takeshima H, Iino M, Takekura H, Nishi M, Kuno J, Minowa O, Takano H, Noda T. 1994. Excitation–contraction uncoupling and muscular degeneration in mice lacking functional skeletal muscle ryanodine-receptor gene. Nature 369:556–559.

Toppin PJ, Chandy TT, Ghanekar A, Kraeva N, Beattie WS, Riazi S. 2010. A report of fulminant malignant hyperthermia in a patient with a novel mutation of the CACNA1S gene. Can J Anaesth 57:689–693.

Trendelensburg AU, Meyer A, Rohner D, Boyle J, Hatakeyama S, Glass DJ. 2009. Myostatin reduced Akt/TORC1/p70S6K signaling, inhibiting myoblast differentiation and myotube size. Am J Physiol Cell Physiol 296:C1258–C1270.

Treves S, Jungbluth H, Muntoni F, Zorzato F. 2008. Congenital muscle disorders with cores: the ryanodine receptor calcium channel paradigm. Curr Opin Pharmacol 8:319–326.

Treves S, Vukcevic M, Griesser J, Franzini-Armstrong C, Zhu MX, Zorzato F. 2010. Agonist-activated Ca2+ influx occurs at stable plasma membrane and endoplasmic reticulum junctions. J Cell Sci 123:4170–4181.

Van Petegem F. 2012. Ryanodine receptors: structure and function. J Biol Chem 287:31624–31632.

Vega AV, Ramos-Mondragon R, Calderon-Rivera A, Zarain-Herzberg A, Avila G. 2011. Calcitonin gene-related peptide restores disrupted excitation–contraction coupling in myotubes expressing central core disease mutations in RyR1. J Physiol 589:4649–4669.

Wilmshurst JM, Lillis S, Zhou H, Pillay K, Henderson H, Kress W, Muller CR, Ndondo A, Cloke V, Cullup T, Bertini E, Boennemann C, et al. 2010. RYR1 mutations are a common cause of congenital myopathies with central nuclei. Ann Neurol 68:717–726.

Zhou H, Jungbluth H, Sewry CA, Feng L, Bertini E, Bushby K, Straub V, Roper H, Rose MR, Brockington M, Kinali M, Manzur A, et al. 2007. Molecular mechanisms and phenotypic variation in RYR1-related congenital myopathies. Brain.

Zhou H, Lillis S, Loy RE, Ghassemi F, Rose MR, Norwood F, Mills K, Al-Sarraj S, Lane RJ, Feng L, Matthews E, Sewry CA, et al. 2010. Multi-minicore disease and atypical periodic paralysis associated with novel mutations in the skeletal muscle ryanodine receptor (RYR1) gene. Neuromuscul Disord 20:166–173.

Zhou H, Yamaguchi N, Xu L, Wang Y, Sewry C, Jungbluth H, Zorzato F, Bertini E, Muntoni F, Meissner G, Treves S. 2006. Characterization of recessive RYR1 mutations in core myopathies. Hum Mol Genet 15:2791–2803.

Zhu CH, Mouly V, Cooper RN, Mamchaoui K, Bigot A, Shay JW, Di Santo JP, Butler-Browne GS, Wright WE. 2007. Cellular senescence in human myoblasts is overcome by human telomerase reverse transcriptase and cyclin-dependent kinase 4: consequences in aging muscle and therapeutic strategies for muscular dystrophies. Aging Cell 6:515–523.